ISSN 1870-4069

CAD Design of a Robotic Thumb of 4 DOF

Luis Fernando Dzul-Maldonado, Eduardo Morales-Sánchez

Instituto Politécnico Nacional,
Centro de Investigación en Ciencia Aplicada y Tecnología Avanzada,
Querétaro,
Mexico

ldzulm2200@alumno.ipn.mx, emoraless@ipn.mx

Abstract. This paper presents a comprehensive study on the design and development of a robotic thumb that closely emulates the natural range of motion and functionality of the human thumb. Careful consideration is given to the thumb's anatomy, including the bones (metacarpal, proximal phalanx, and distal phalanx) and joints (carpometacarpal, metacarpophalangeal, and interphalangeal). Anthropometric proportions and biomechanical principles are incorporated to ensure accuracy and realism including them in a Kinematic Model. CAD software is utilized for modeling and simulation, incorporating four degrees of freedom (DOF) for two movements of flexion extension, the abduction adduction, and the opposition of the thumb. The modeling is divided in the design of the phalanges and the metacarpal section. Comparative analysis against established benchmarks and reported ranges of motion validates the design with the help of a simulation program through the Kinematic Model, demonstrating that the robotic thumb matches or exceeds natural ranges of movement. These findings highlight the potential of the robotic thumb for real-world applications. In conclusion, this paper presents a successful design and development of an anthropomorphic robotic thumb that replicates the range of motion and characteristics of the human thumb.

Keyword: Robotic hand, thumb, degrees of freedom.

1 Introduction

Human hands are extremely complex due to their ability to perform a wide variety of tasks, from handling delicate objects to performing complex and precise movements. Researchers have tried to model those functional features for robotic multififingered grippers since the mid-eighties (Nanayakkara et al., 2017) and the anthropomorphic robotic dexterous hand has become one of the most important researching fields on humanoid robots (Wang et al., 2012), and a crucial element of the robotic hand design is the thumb.

Robotic thumbs play a crucial role in the development of robotic hands as they mimic the dexterity and functionality of the human thumb. By incorporating a robotic thumb with multiple degrees of freedom (DOF) into a robotic hand, engineers and researchers can enhance the hand's overall functionality, adaptability, and versatility. Examples of robotic thumbs include the Gifu Hand III (Tetsuya et al., 2002) which

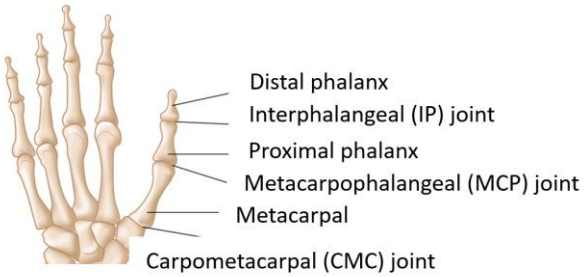

Fig. 1. Bones and joints of the human thumb [1].

possesses a 4 DOF thumb, the multiarticulated hand (Ramos, 2021), with a thumb of 3 DOF, the EthoHand (Konnaris, 2016) with a ball articulation actuated with tendons, or the thumb developed by Prudencio et al. (2014) with 3 DOF.

There is also use of soft robotics like the BCL-13 (Zhou et. al., 2018) and the RBO Hand 2 (Deimel and Brock, 2016). There also are underactuated designs like the thumbs of the SCCA Hand (Wiste, Tuomas et. al, 2017) and the Adam's hand (Zappatore Giovanni et. al, 2017) that keep rigid mechanisms and others that use tendons like the Highly Biomimetic Anthropomorphic Robotic Hand (Xu, Zhe and Todorov, Emanuel, 2016).

The design and development of robotic thumbs involve careful consideration of anthropometry, biomechanics, and kinematics to achieve optimal performance. By emulating the structure and movements of the human thumb, robotic thumbs can provide increased dexterity and enable the hand to perform a wide range of tasks in various environments.

The objective of this paper is to design, analyze, and evaluate a robotic thumb with anthropometric proportions and 4 DOF using the Fusion 360 CAD program, with a focus on generating opposition and adduction movements. The paper aims to provide a comprehensive understanding of the design process, functionality, and potential applications of the robotic thumb in the development of robotic hands.

2 Thumbs Anatomy

The human thumb is a vital component of hand functionality, characterized by its unique structure and mobility. Understanding the anatomy of the human thumb's bones and joints is crucial to generate a design which imitates its anthropomorphy and anthropometry. There are 3 bones inside the thumb (see Fig. 1): the metacarpal bone, where the thumb originates and connects the thumb to the wrist. It is short and robust, allowing for stability and strength during grasping motions.

The proximal phalanx, the first phalanx of the thumb, located closest to the metacarpal bone. It is responsible for the thumb's pivotal movement and flexion. And the distal phalanx which forms the tip of the thumb. It provides support and precision for grasping objects.

As for the joints there are also 3 in the thumb (see Fig. 1) those being: the carpometacarpal joint (CMC), located at the base of the thumb, where the metacarpal

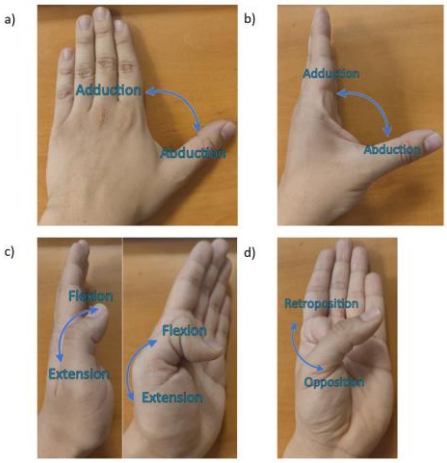

Fig. 2. Movements of the thumb. a) The radial abduction/adduction of the thumb. b) The palmar abduction/adduction of the thumb. c) The flexion/extension of the IP and MCP thumb joints. d) The opposition/retroposition of the thumb.

bone connects to the carpal bones of the wrist. The metacarpophalangeal joint (MCP) that connects the metacarpal bone to the proximal phalanx. It permits flexion, extension, and abduction-adduction movements of the thumb. And the interphalangeal joint (IP), present between the proximal and distal phalanges. It allows for flexion and extension movements, contributing to the thumb's grasping capabilities (see Fig. 2).

The carpometacarpal (CMC) joint primarily facilitates abduction and adduction of the thumb. Abduction refers to the motion of the thumb away from the second metacarpal bone, while adduction signifies the opposite movement. These motions occur in two planes: palmar and dorsal. Radial abduction-adduction involves the thumb moving parallel to both the radius and the palm of the hand, with a relatively smaller range of motion. In contrast, palmar abduction-adduction occurs in a plane perpendicular to the palm of the hand.

These bones and joints collectively provide the thumb with its remarkable dexterity and versatility, allowing for a wide range of movements and precision in object manipulation. Understanding the anatomical structure of the human thumb serves as a valuable reference point for designing and developing robotic thumbs with comparable functionalities.

3 Design Methodology

In the realm of robotic hand design, their elements can be categorized into two groups based on their actuators: tendon-driven and rigid mechanics-driven. Tendon-driven systems utilize cables to generate movements, while rigid mechanics-driven systems employ gears.

The robotic thumb discussed in this paper falls into the latter category and is equipped with four actuated degrees of freedom (DOF). This requires careful

Table 1. Anthropometric measurements of the thumb according to the norm DIN 33402 (DIN, 2020).

Dimensions (cm)	Percentile					
	Men			Women		
	5%	50%	95%	5%	50%	95%
(34) Thumb Length	6.0	6.7	7.6	5.2	6.0	6.9
(37) Thumb Width	2.0	2.3	2.5	1.6	1.9	2.1
(39) Hand Length with Thumb	9.8	10.7	11.6	8.2	9.2	10.1
(40) Hand Length without Thumb	7.8	8.5	9.3	7.2	8.0	8.5

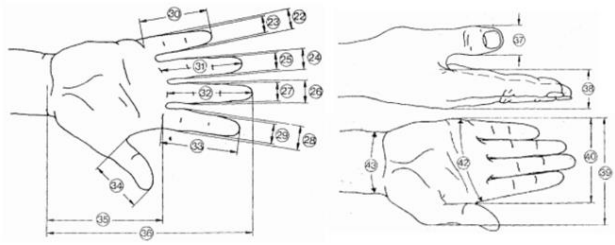

Fig 3. Anthropometric measurements of the hand according to norm DIN 33402 (DIN, 2020).

consideration of selecting compact motors that can fit within the thumb's confines and dividing the design into separate parts for independent movement and assembly.

The method used to design the robotic thumb can be divided in three sections, the design requirements, the development of the phalanges, and the design of the metacarpal bone, both of those must keep the anthropometry of the thumb, following the DIN 33402 norm (DIN, 2020) (see Table 1 and Fig. 3).

3.1 Design Requirements

To demonstrate the anthropomorphic qualities of the robotic finger, three key factors are essential: joint structure, dexterity, and appearance. The joint structure entails utilizing phalanges and joints that closely resemble those found in a human finger. Dexterity encompasses the finger's ability to mimic natural human movements, aligning with the initial design concept. Additionally, the appearance of the robotic finger must closely resemble that of a human thumb.

To achieve the desired range of motion, the robotic finger is designed with four actuated degrees of freedom (DOF). These include opposition, abduction-adduction in both palmar and radial planes, and flexion-extension of the metacarpophalangeal (MCP) and interphalangeal (IP) joints.

The joint structure incorporates a division of the metacarpal bone to facilitate opposition and abduction-adduction movements while maintaining the human thumb's appearance. The distance between the divisions is set to the minimum allowed by the actuators to ensure a natural appearance.

i	a_i	α_i	d_i	θ_i
a	0	-90	0	-90
b	0	0	55	0
1	13.25	0	0	θ_1
c	31.96	90	-2.25	0
2	0	0	0	θ_2
d	34.472	-90	0	90
3	31.25	0	0	θ_3
4	45	0	0	θ_4
5	30	0	0	0

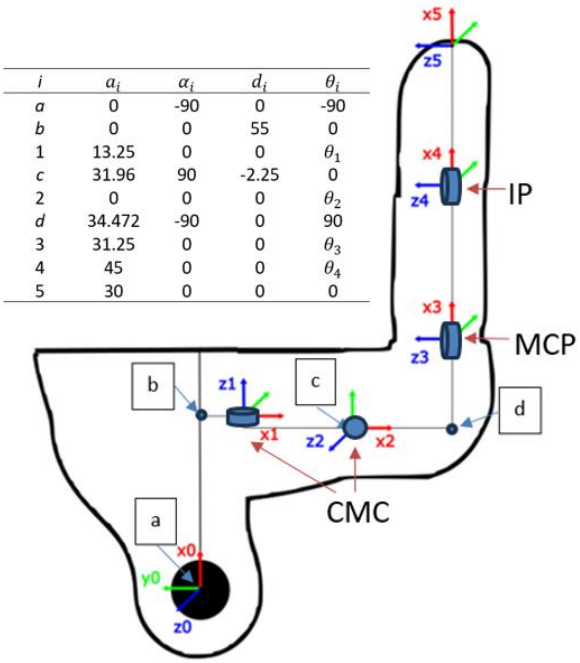

Fig 4. Denavit Hartenberg (DH) Kinematic Model. The DH parameters are shown in the table above. There are 4 joints (i = 1,2,3,4) i = 1 and 2 correspond to the CMC joint, i = 3 to the MCP joint and i = 4 to the IP joint, i = 0 is the location of the wrist and there are also auxiliary parameters used for transformations between joints (i = *a,b,c,d*).

In terms of the mechanical design, the robotic finger incorporates a transmission system utilizing rigid links. The chosen actuators for this design are the n20 micromotors, which are equipped with gearboxes. These micromotors, with dimensions of 33.5 x 12.1 x 10 mm, are strategically positioned within the proximal phalanx and the two parts of the metacarpal bone, leaving one to be coupled to a robotic hand.

By addressing these factors, the robotic finger achieves a remarkable level of anthropomorphism, closely resembling the joint structure, dexterity, and appearance of a human thumb. The design's integration of the transmission system using n20 micromotors ensures the finger's effective actuation and movement capabilities.

3.2 Kinematic Model of the Robotic Thumb

To mathematically represent the movements and positions of the robotic thumb, a kinematic model was developed. The kinematic model outlines the relationships between joint angles and the resulting position and orientation of the thumb. It is crucial for understanding and predicting the thumb's behavior during various motions.

The Denavit-Hartenberg (DH) parameters, shown in Fig. 4, were employed to describe the transformations between adjacent links of the robotic thumb. These

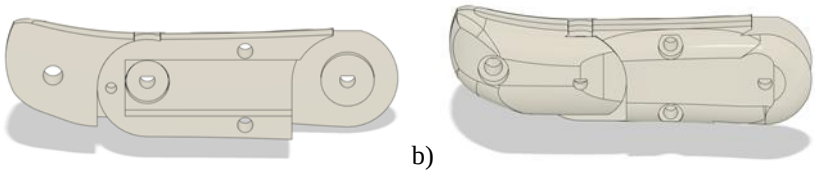

a) b)

Fig. 5. CAD design of the thumb phalanges with lateral view of a) the inside of the thumb, where a compartment for the actuator can be seen, and b) the assembled phalanges of the thumb.

parameters include link lengths, joint angles, and other geometric information that define the kinematic properties of the thumb.

The kinematic model serves as a tool for validating the design of the robotic thumb. By simulating movements using the model, we could ensure that the designed structure facilitates the intended range of motion and functionality, this also permitted us to optimize the design parameters to achieve optimal performance in simulation. This involved adjusting metacarpal lengths, while refining the overall structure to enhance the thumb's dexterity.

The Forward Kinematics were calculated by the multiplication of the transformation matrices (equation 1). These equations enable us to determine the end-effector pose of the thumb:

$$T_5 = T_a \times T_b \times T_{01} \times T_c \times T_{12} \times T_d \times T_{23} \times T_{34} \times T_{45}\,, \tag{1}$$

where:

$T_{01}, T_{12}, T_{23}, T_{34}$ are transformation matrices for respective joints.

And

T_a, T_b, T_c, T_d are auxiliary parameters used for transformations between joints.

3.3 Phalanges CAD Design

The human thumb has two phalanges: the proximal and the distal. To ensure accurate design of the robotic thumb, it is essential to establish precise measurements for the joint distances. In this case, the distance between the joints is set at 45 mm, while the length of the distal phalanx measures 30 mm, the diameter of both of a maximum of 25 mm to be in the range of the DIN 33402 norm, also specified in the Kinematic Model.

By knowing the joint positions, it becomes possible to create the silhouette of the human finger, divided into the two phalanges. These silhouettes are then extruded, and further details are added using a fillet tool.

For the proximal phalanx, which possesses two joints, a compartment is designed to house the micro motor n20. The motor axis is positioned at the center of the interphalangeal joint, enabling the flexion and extension movements of the distal phalanx. The design of the distal phalanx is such that it can be assembled to the proximal phalanx while accommodating the motor within.

Considering the design is intended for additive manufacturing, each phalanx needs to be divided into two parts to allow for assembly and integration of the motor, it is also needed to design the unions where the phalanges will be assembled (see Fig. 5a).

Table 2. Measurements of the robotic thumb by their links, including the maximum dimensions of the links between each joint and the range of movements angle of each joint.

Link	**Measurements**			
	Dimensions (mm)		Range of Movement	
	Max Length	Max Width	Joint	Angle
Distal Phalanx	30	25	IP	-15° - 90°
Proximal Phalanx	45	25	MCP	-15° - 78°
Metacarpal bone (abduction)	50	45	CMC	0° - 69°
Metacarpal bone (opposition)	45	45	CMC	-18° - 80°

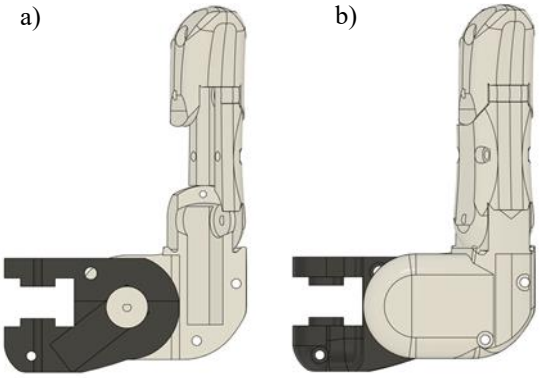

Fig. 6. CAD design of the thumb phalanges with top view of a) the inside of the thumb, where the actuators compartments can be seen, and b) the assembled thumb.

3.4 Metacarpal Bone CAD Design

To design the metacarpal bone section there needs to be a division of the shape of the thumb to generate both the opposition and the adduction-abduction movement, the last needed to be able to be generated in both the radial and palmar plane of the hand, leaving the opposition movement first in the base of the thumb followed by the adduction-abduction. The design needs to consider the hand to include a motor inside it for the opposition, while the next link of the thumb to generate the adduction-abduction, and the next link to do the flexion-extension of the MCP joint.

To achieve this, the design required an approximation of the shape of the hand as a reference. Using the DIN 33402 norm, the length of the hand was acquired and half of it was used for the length of the thumb inside the hand, followed by separating that half from the rest of the hand. By closely referring to the shape of an actual human thumb, the design could be created.

Table 3. Table of comparison of the design of the robotic thumb proposed and the benchmark ranges of movement (ROM) based on the average values reported by Barakat et al. (2013). The proposed robotic thumb design demonstrates ROM that closely align with or exceed these benchmarks. *In the mechanical design of the robotic thumb the abduction works in both palmar and radial planes. **The Expected Kapandji grade of 10 refers to the thumb ROM when added to a complete robotic hand.

Joint	Average Range of Movement (Barakat et al., 2013)	Proposed Robotic Thumb Design
IP Joint	Flexion: 88°	Flexion: 90°
	Extension: 12°	Extension: 15°
MCP Joint	Flexion: 60°	Flexion: 78°
	Extension: 8.1°	Extension: 15°
CMC Joint	Palmar Abduction: 61.2°	*Abduction: 69°
	Radial Abduction: 62.9°	
	Kapandji grade: 9	**Expected Kapandji grade: 10

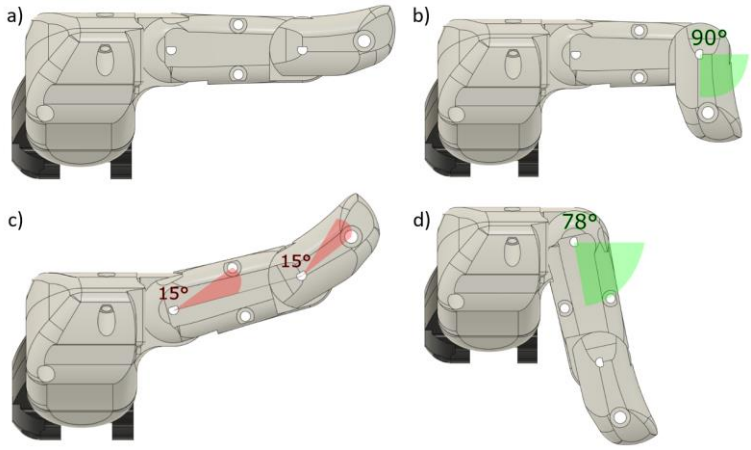

Fig. 7. CAD range of movement of the thumb a) resting position; b) flexion of the IP joint with a maximum range of 90°; c) extension of the IP and MCP joints with a maximum range of 15° each; and d) flexion of the MCP joint with a maximum range of 78°.

The design process for the metacarpal bone section, began by rotating the previously designed phalanges along their axis to simulate the natural resting position of the thumb, achieving a 30° angle. Subsequently, a top view design was created referring to the kinematic model, to replicate the thumb's shape in the horizontal plane of the hand, giving dimensions of 50 mm parallel to the axis of the phalanges and 90 mm perpendicular to it.

This was followed by generating the side and back views of the thumb in perpendicular planes with a depth of 45 mm. By combining these views, an approximate shape of the thumb was formed, capturing its essential characteristics. To add finer details, a fillet tool was employed, enhancing the realism and accuracy of the design.

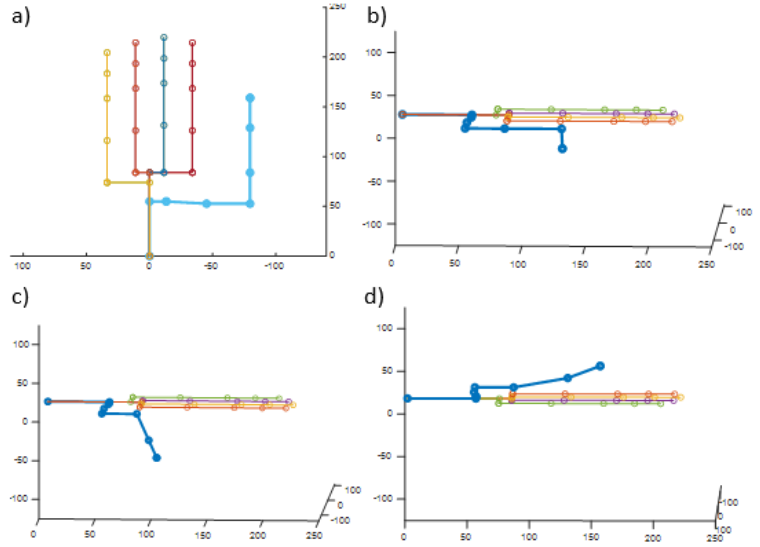

Fig. 10. MATLAB range of movement of the thumb a) resting position; b) flexion of the IP joint with a maximum range of 90°; c) flexion of the MCP joint with a maximum range of 78°; and d) extension of the IP and MCP joints with a maximum range of 15° each.

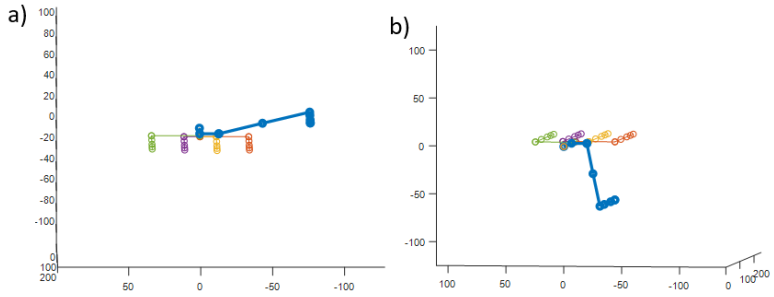

Fig. 11. MATLAB range of movement of the CMC joint a) retroposition with a maximum of 18°; b) resting position; and c) opposition with a maximum of 80°.

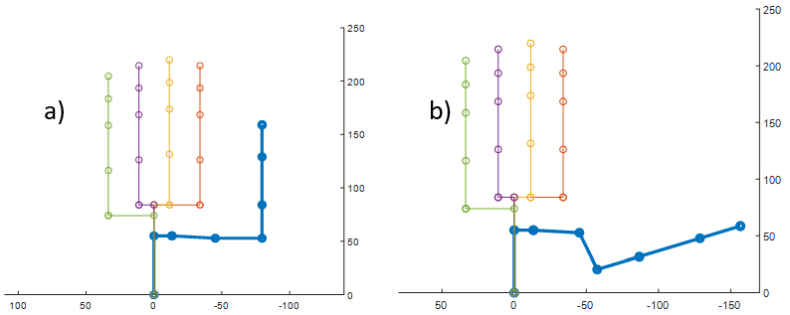

Fig. 12. MATLAB range of movement of the thumb phalanges a) rest position; and b) abduction of the CMC joint with a maximum range of 69°.

After generating an approximate shape, the measurements of the motors n20, were considered to create the divisions of the links of the thumb, so compartments were created starting from the motor used for the MCP flexion-extension and ending by the opposition motor. These compartments were made considering the limited space of the thumb. Finally, the shape was divided in two links of 45 mm each perpendicular to the phalanges axis (see Table 2), by using the motors axis in reference and considering the assembly of the parts to generate the movement (see Fig. 6).

4 Range of Motion

The average ranges of movement reported by Barakat et al. (2013) served as a benchmark for comparison. According to their findings, the average ranges of movement for the IP joint were 88° of flexion and 12° of extension, while the MCP joint exhibited 60° of flexion and 8.1° of extension. The CMC joint demonstrated a palmar abduction of 61.2°, retroposition of 31°, and radial abduction of 62.9°.

In our simulated CAD assembly, we carefully assessed the range of movement for each joint. The results revealed promising outcomes, with the designed thumb showcasing ranges of movement that closely aligned with the average values reported in the literature. Specifically, the IP joint demonstrated a flexion range of 90° and an extension range of 15°. The MCP joint exhibited a flexion range of 78° and an extension range of 15° (see Fig. 7). The CMC joint displayed an opposition range of 80°, retroposition range of 18° (see Fig. 8), and abduction (both radial and palmar) range of 69° (see Fig. 9).

The similarities between our simulated ranges and the reported average ranges of movement indicate that our design effectively emulates the natural movement capabilities of the human thumb. However, it is important to note that these results are based on a simulated CAD assembly, and further validation is required through physical prototyping and experimentation involving human participants. Such validation studies would provide more accurate insights into the actual performance and usability of the designed thumb (see Table 3).

4.1 Range of Motion Validation through Kinematic Simulation in MATLAB

To validate the accuracy of the ROM, a simulation was conducted using the forward kinematics equations with the Kinematic Model. The simulated range of motion was compared with the actual range obtained from the CAD design, ensuring the consistency and reliability with the kinematic model.

The kinematic model aids in predicting the workspace of the robotic thumb, indicating the range of positions and orientations it can achieve. This information is crucial for future applications in control, it also allows us to assess the feasibility of the design before advancing to the physical prototyping stage. It also helped verify no potential issues such as joint limitations, collisions, or singularities (see Fig. 10-12).

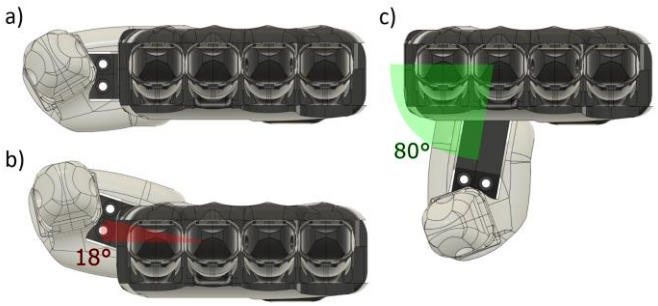

Fig. 8. CAD range of movement of the CMC joint a) retroposition with a maximum of 18°; b) resting position; and c) opposition with a maximum of 80°.

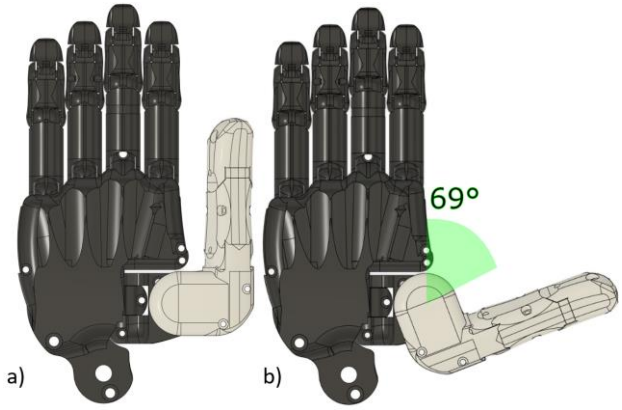

Fig. 9. CAD range of movement of the thumb phalanges a) rest position; and b) abduction of the CMC joint with a maximum range of 69°.

5 Conclusion

A successful design was presented for a robotic thumb capable of achieving a wide range of movements, closely resembling the anthropomorphic features of a human thumb. The design encompassed all essential ranges of motion, including flexion, extension, abduction, adduction, and opposition, using 4 DOF, while maintaining accurate anthropometry.

The designed robotic thumb stands as a significant contribution, being among the few designs to successfully integrate four degrees of freedom (DOF) into a thumb while adhering to anthropometric measurements. This achievement is made possible through a meticulously crafted design based on gear-driven mechanics, enabling the thumb to replicate intricate human-like movements including opposition, flexion, extension, as well as palmar and radial abduction-adduction.

The design process involved meticulous considerations, such as dividing the thumb's shape to accommodate opposition and adduction-abduction movements, as well as selecting appropriate motors and creating compartments within the thumb for their

integration. The resulting design demonstrates the potential for constructing the thumb through 3D printing and subsequent assembly.

The simulated ranges of movement for each joint were evaluated and compared to the designed ranges, confirming the effectiveness of the kinematic model in accurately representing the thumb's motion capabilities.

By achieving a thumb design with human-like functionality and appearance, this work sets the stage for future advancements in robotic hand development. The designed thumb can be seamlessly integrated into a robotic hand system, enhancing its dexterity and grasp capabilities.

Overall, this research showcases a promising step towards the realization of highly functional and lifelike robotic hands, opening doors for numerous applications in fields such as prosthetics, human-robot interaction, and industrial automation. Future work can focus on the manufacturing and assembly of the designed thumb, as well as exploring its integration into a complete robotic hand system for comprehensive functionality and performance evaluation.

References

1. Americam Academic of Orthopedic Surgeon.: Thumb Fractures https://orthoinfo.aaos.org/en/diseases--conditions/thumb-fractures/
2. Barakat, M. J., Field, J., Taylor, J.: The range of movement of the thumb. Sage Journal, vol. 8, no. 2, pp. 179–182 (2013) doi: 10.1007/s11552-013-9492-y
3. Cabibihan, J. J., Alkhatib, F., Mudassir, M., Al-Kwifi, O. S., Diab, K., Mahdi, E.: Suitability of the openly accessible 3D printed prosthetic hands for war-wounded children. Frontiers in Robotics and AI, vol. 7 (2021) doi: 10.3389/frobt.2020.594196
4. Cotugno, G., Althoefer, K., Nanayakkara, T.: The role of the thumb: Study of finger motion in grasping and reachability space in human and robotic hands. IEEE Transactions on Systems, Man, and Cybernetics: Systems, vol. 47, no. 7, pp. 1061–1070 (2016) doi: 10.1109/TSMC.2016.2531679
5. Drake, R. L., Vogl, A. W., Mitchell, A. W.: Gray anatomía para estudiantes. 3a. ed., Barcelona: Elsevier (2015)
6. El-Sawah, A., Georganas, N. D., Petriu, E. M.: Finger inverse kinematics using error model analysis for gesture enabled navigation in virtual environments. In: 2006 IEEE International Workshop on Haptic Audio Visual Environments and their Applications, HAVE´06, pp. 34–39 (2006) doi: 10.1109/HAVE.2006.283786
7. Prudencio, A., Morales, E., García, M. A., Lozano, A.: Anthropometric and anthropomorphic features applied to a mechanical finger. In: Intelligent Robotics and Applications: 7th International Conference, ICIRA´14, Springer International Publishing, vol. 8917, pp. 254-265 (2014) doi: 10.1007/978-3-319-13966-1_26
8. Ramos, M.: Diseño y construcción de una mano robótica humanoide multiarticulada. Trabajo de tesis, Centro de Investigación en Ciencia Aplicada y Tecnología Avanzada-IPN, Unidad Querétaro (2021)
9. Reyes, A., Morales, E.: Generación del agarre de precisión mediante dedos robóticos multiarticulados con características antropométricas y antropomórficas basado en mecanismos planares de 4 barras. Pistas Educativas, no. 130, Tecnológico Nacional de México en Celaya (2018)
10. Mouri, T., Kawasaki, H., Yoshikawa, K., Takai, J., Ito, S.: Anthropomorphic robot hand: gifu hand III. Semantic Scholar, pp. 1288–1293 (2002)

11. Wang, H., Fan, S., Liu, H.: An anthropomorphic design guideline for the thumb of the dexterous hand. In: IEEE International Conference on Mechatronics and Automation, pp. 777–782 (2012)
12. Zhou, J., Yi, J., Chen, X., Liu, Z., Wang, Z.: BCL-13: A 13-DOF soft robotic hand for dexterous grasping and in-hand manipulation. IEEE Robotics and Automation Letters, vol. 3, no. 4, pp. 3379–3386 (2018) doi: 10.1109/LRA.2018.2851360
13. Konnaris, C., Gavriel, C., Thomik, A. A., Faisal, A. A.: Ethohand: A dexterous robotic hand with ball-joint thumb enables complex in-hand object manipulation. In: 2016 6th IEEE international conference on biomedical robotics and biomechatronics (BioRob), pp. 1154–1159 (2016) doi: 10.1109/BIOROB.2016.7523787
14. Deimel, R., Brock, O.: A novel type of compliant and underactuated robotic hand for dexterous grasping. International Journal of Robotics Research, vol. 35, no. 1-3, pp. 161–185 (2016) doi:10.1 177/0278364915592961
15. Deutsche Institut für Normung: DIN 33402-2:2020. DIN. ICS: 13.180 (2020)
16. Xu, Z., Todorov, E.: Design of a highly biomimetic anthropomorphic robotic hand towards artificial limb regeneration. In: 2016 IEEE International Conference on Robotics and Automation (ICRA), pp. 3485–3492 (2016) doi: 10.1109/ICRA.2016.7487528
17. Zappatore, G. A., Reina, G., Messina, A.: Adam's Hand: An underactuated robotic end-effector. In: Advances in Italian Mechanism Science: Proceedings of the First International Conference of IFToMM, Springer International Publishing, pp. 239–246 (2017) doi: 10.10 07/978-3-319-48375-7_26
18. Wiste, T., Goldfarb, M.: Design of a simplified compliant anthropomorphic robot hand. In: 2017 IEEE International Conference on Robotics and Automation, pp. 3433–38 (2017) doi: 10.1109/ICRA.2017.7989391